

The variations of VOCs based on the policy change of Omicron in traffic-hub city Zhengzhou

Bowen Zhang^{1,3}, Dong Zhang^{2,3}, Zhe Dong^{2,3}, Xinshuai Song^{1,3}, Ruiqin Zhang^{1,3},
Xiao Li^{1,3,*}

¹School of Ecology and Environment, Zhengzhou University, Zhengzhou 450001,
China

²College of Chemistry, Zhengzhou University, Zhengzhou 450001, China

³Institute of Environmental Sciences, Zhengzhou University, Zhengzhou 450001,
China

Abstract: Online volatile organic compounds (VOCs) were monitored before and after the Omicron policy change at an urban site in polluted Zhengzhou from December 1, 2022, to January 31, 2023. The characteristics and sources of VOCs were explored. The daily average concentration of PM_{2.5} and total VOCs (TVOCs) ranged from 53.5 to 239.4 $\mu\text{g}/\text{m}^3$ and from 15.6 to 57.1 ppbv with an average value of $111.5 \pm 45.1 \mu\text{g}/\text{m}^3$ and 36.1 ± 21.0 ppbv, respectively during the entire period. The values of PM_{2.5} and TVOCs in Case 2 (pollution episode after the abolishment of “Nucleic Acid Screening Measures for all staff” policy) were 1.3 and 1.8 times of the values in the Case 1 (pollution episode during “Nucleic Acid Screening Measures for all staff” policy). The concentration of TVOCs in Case 1 and Case 2 were 48.4 ± 20.4 and 67.6 ± 19.6 ppbv, respectively, increased by 63% and 188% compared with values during clean days. Alkanes were found to be the most abundant compounds during the entire period. Equivalent volume contribution of halogenated hydrocarbon and oxygenated VOCs (15%) were found the most in Case 2, followed by alkenes (10%). Though the volume contributions of aromatics were the lowest (6% in Case 1 and 7% in Case 2), the highest increasing ratio was found from clean days to polluted episodes. Positive Matrix Factor model results showed that the main source of VOCs during the observation period was industrial emissions, which accounted for 32% of the TVOCs, followed by vehicular emission (27%) and combustion (21%). In Case 1, industrial emissions constituted the largest contributor, accounting for 32% of the total VOCs. In Case 2, however, the share of vehicular emission source increased to 33%, becoming the primary source of VOCs. Secondary organic aerosol formation potential (SOAP) values were 37.6 and 65.6 $\mu\text{g}/\text{m}^3$ in Case 1 and Case 2, respectively. In Case 1, industrial source accounted for the overwhelming majority (63%, 23.8 $\mu\text{g}/\text{m}^3$), while vehicular source, as the second

34 largest source, accounted for only 18%. In Case 2, the distribution of contributions is
35 more uniform, with solvent usage source and fuel evaporation source accounting for
36 the majority of SOAP, at 32% (20.9 $\mu\text{g}/\text{m}^3$) and 26% (16.8 $\mu\text{g}/\text{m}^3$), respectively.
37 Industrial source and solvent usage continue to be the main contributors to SOAP on
38 clean days. It is crucial to prioritize the regulation of emissions from industrial and
39 solvent-using sectors as a means of curbing $\text{PM}_{2.5}$ pollution in Zhengzhou. Additionally,
40 it is imperative to consider the impact of rising vehicular emissions on air quality.

41

42 **Keywords: Volatile organic compounds; Pollution episode; Source apportionment;**

43 1. Introduction

44 Volatile organic compounds (VOCs) in the atmosphere have high reactivity and
45 can react with nitrogen oxides (NO_x) to form a series of secondary pollutants such as
46 ozone (O₃) and secondary organic aerosol (SOA), resulting in regional air pollution (Li
47 et al., 2019; Hui et al., 2020). The problem of O₃ pollution has been plaguing major
48 urban agglomerations in China (Zheng et al., 2010; Li et al., 2014; Wang et al., 2017).
49 SOA is an important component of fine particulate matter (PM_{2.5}) and contributes
50 significantly to haze pollution (Liu et al., 2019). PM_{2.5} remains the most significant air
51 pollutant in many Chinese cities for years (Shao et al., 2016; Wu et al., 2016). In
52 addition, VOCs, represented by the benzene homologues, can cause damage to kidneys,
53 liver, and nervous system of humans when they enter the body (Zhang et al., 2018).

54 Studies have shown that the most common VOC components in China are alkanes,
55 olefins, aromatic hydrocarbons, oxygenated VOCs (OVOCs), and halogenated
56 hydrocarbons, among which alkanes are the most abundant species (Liu et al., 2020;
57 Zhang et al., 2021a). VOCs in the atmosphere have a wide range of sources, and VOCs
58 in different regions are affected by multiple factors such as local geography, climate,
59 and human activities (Mu et al., 2023; Zou et al., 2023). The above reasons lead to
60 significant regional and seasonal differences in the characteristics of VOCs (Song et al.,
61 2021). For example, the annual average concentration of VOCs in the coastal
62 background area of the Pearl River Delta is 9.3 ppbv. The seasonal variation trend of
63 VOCs is high in autumn and winter and low in summer (Yun et al., 2021). In contrast,
64 the average VOC concentration in autumn and winter in Beijing was 22.6 ± 12.6 ppbv,
65 and the VOC concentration in the winter heating period was twice that in the autumn
66 non-heating period (Niu et al., 2022).

67 Moreover, the sources of VOC components in different regions are also related to
68 the local industrial structure and living habits. In rural areas of North China Plain in
69 winter, it is found that the SOA formation potential (SOAP) of VOCs under low NO_x
70 conditions is significantly higher than that under high NO_x conditions, and the increase
71 of aromatic hydrocarbon emissions caused by coal combustion is the main reason for
72 the higher SOAP in winter (Zhang et al., 2020). Li et al. (2022) found that the average
73 increased concentration of acetylene was 4.8 times from autumn to winter in the
74 Guanzhong Plain, indicating that fuel combustion during the heating period in winter
75 has a significant impact on the composition of VOCs. In contrast, continuous

76 observations conducted by Zhou et al. (2022) in the suburbs of Dongguan in summer
77 found that industrial solvent usage, liquefied petroleum gas (LPG) and oil and gas
78 volatilization were the main sources of VOCs. The results highlighted a wide variation
79 of characteristics, sources and chemical reactions of VOCs in the atmosphere, thus it is
80 necessary to investigate VOCs in different cities when formulating control measures.

81 Zhengzhou, as the capital of Henan Province, is an important transportation hub
82 and economic center in the Central Plains region. Zhengzhou is currently facing
83 significant air pollution problems, with the Air Quality Index at the bottom of the
84 national ranking of 168 cities for many years. In January 2023, for example, the number
85 of polluted days with PM_{2.5} as the primary pollutant was 17, and the daily average value
86 of PM_{2.5} reached a maximum of 298 µg/m³
87 ([https://www.aqistudy.cn/historydata/daydata.php?city=%E9%83%91%E5%B7%9E](https://www.aqistudy.cn/historydata/daydata.php?city=%E9%83%91%E5%B7%9E&month=202301)
88 [&month=202301](https://www.aqistudy.cn/historydata/daydata.php?city=%E9%83%91%E5%B7%9E&month=202301), Accessed Jan 2024), which is almost 300% higher than the Chinese
89 daily average standard (grade II, 75 µg/m³). The studies of VOCs were carried out in
90 Zhengzhou in recent years, which focused on the characteristics and sources of VOCs
91 during pollution episodes (Lai et al., 2024) or before the coronavirus epidemic outbreak
92 (Li et al., 2020; Zhang et al., 2021b). While some atmospheric VOCs studies involving
93 the impact of Covid-19 lockdown have been performed in India (Singh et al., 2023a),
94 in China (e.g., Pei et al., 2022; Jensen et al., 2023; Zuo et al., 2024), or with respect to
95 toluene, benzene, m/p-xylene and ethylbenzene only (e.g., Sahu et al., 2022; Singh et
96 al., 2023b), a gap persisted in the investigation of VOCs due to the impact of
97 abolishment of China's zero-policy. In addition, there have been some studies
98 discussing the impact of human factors on air pollution during and after the outbreak
99 of the Coronavirus disease (e.g., Ma et al., 2022; Jiang et al., 2023; Song et al., 2023),
100 but as mentioned earlier, only a few studies with in-depth exploration of the changes in
101 VOCs and none dealing with ending the zero-Covid policy during Omicron variant
102 infection period.

103 In this study, a continuous online observation of VOCs in polluted winter at an
104 urban site was carried out, which covered the abolishment of lockdown measures in
105 Zhengzhou. China lifted the zero-COVID strategies, notably by announcing the '10
106 measures' about the optimization of COVID-19 rules on 7 December 2022
107 (http://www.news.cn/politics/2022-12/07/c_1129189285.htm, Accessed Jan 2024),
108 which led to significant changes in social activities. After that, China experiences a
109 nationwide outbreak of COVID-19. Our research primarily concentrates on the period

110 dominated by COVID-19 Omicron variant, where they demonstrate notable differences
111 from the early virus strains (i.e., original SARS-CoV-2 virus and Delta) in terms of
112 geographical transmission, the scale of the infected population, and symptom
113 manifestation (Petersen et al., 2022; Merino et al., 2023). A two-month-long lockdown
114 measure was applied to after first Omicron case of student in Zhengzhou University
115 was confirmed on October 8, 2022. Lockdown measure was abolished from the
116 beginning of December in 2022, which resulted in a sharp increase of Omicron-infected
117 people and a decrease in daily social production activities. In fact, the “Nucleic Acid
118 Screening Measures for all staff” policy was also canceled at 8 October in 2022. People
119 are basically homebound after the lifting of the lockdown policy due to infection or fear
120 of infection of Omicron. The resumption of normal production and livelihoods was
121 based on the assumption of herd immunization. **This change is worth exploring in terms
122 of its impact on transportation and industrial production emissions.** Therefore, the
123 characteristics and variations of VOCs during different periods were investigated to
124 assess their impact on the formation of SOA and to provide data support for future
125 pollution control policies in Zhengzhou.
126

127 2. Materials and methods

128 2.1 Sample collection and Chemical analysis

129 The online VOCs observation station is located on the roof of the Zhengzhou
130 Environmental Protection Monitoring Center, which is in the urban area. The sampling
131 site is close to main roads on three sides (150 m away from Funiu Road on the east side,
132 200 m away from Qinling Road on the west side, and connected to Zhongyuan Road
133 on the south side), and surrounded by residential areas and commercial areas without
134 other large nearby stationary sources. The sampling period for this study was from
135 December 1, 2022, to January 31, 2023, which is always the most polluted period in
136 the entire year. Apart from a brief occurrence of rain and snow on December 25, the
137 sampling days were either sunny or cloudy. The wind speed (WS), temperature (Temp)
138 and relative humidity (RH) during this period were 1.3 ± 0.9 m/s, 5.3 ± 3.2 °C and 38.9
139 $\pm 19.0\%$), respectively, similar to the values observed in previous years in Zhengzhou.
140 It is interesting to point out that the sampling period in the present study covered the
141 entire infection period of Omicron in Zhengzhou, including the phase of surge in
142 infected population (Infection period, from 2022.12.01 to 2022.12.31) and restoration
143 of production and livelihood phase (Recovery period, from 2023.1.1 to 2023.1.31 in
144 2023) (Fig. S1, [Chinese Center for Disease Control and Prevention, 2023](#)).

145 The VOCs were measured hourly using a GC-FID/MS (TH-PKU 300 b, Wuhan
146 Tianhong Instruments Co., China). The instrument TH-PKU300b includes electronic
147 refrigeration ultra-low temperature pre-concentration sampling system, analysis system
148 and system control software. The ambient VOCs in the first 5 minutes of each hour
149 were collected by the sampling system and then entered the concentration system.
150 Under low temperature conditions, the VOCs samples collected were frozen in the
151 capillary capture column, and then quickly heated and resolved, so that the compounds
152 entered the analysis system. After separation by chromatographic column, the
153 compounds were monitored by FID and MS detectors. During the detection process,
154 the atmospheric samples collected undergo analysis through two distinct pathways. C2-
155 C5 hydrocarbons are analyzed using FID, while C5-C12 hydrocarbons, halocarbons,
156 and OVOCs are analyzed with a MS detector. After excluding species with missing data
157 exceeding 10%, the detected volatile organic compounds include 29 alkanes, 11 alkenes,
158 17 aromatics, 35 halocarbons, 12 OVOCs, 1 alkyne (acetylene), and 1 sulfide (CS₂)
159 with a total of 106 compounds.

160 The instrument was calibrated per week to ensure the accuracy of VOCs by
161 injecting standard gases with a five-point calibration curve. The detection limit of C2-
162 C5 hydrocarbons ranges from 0.007 to 0.099 ppbv, other hydrocarbons are 0.004–0.045
163 ppbv, halogenated hydrocarbons 0.009-0.099 ppbv, OVOCs and other compounds of
164 0.006–0.095 ppbv. Thirty-two of the monitored VOCs had over 90% observed data
165 greater than the detection limit, and 34 had more than 50% observed data greater than
166 the detection limit.

167 Simultaneous observations at the same site were also carried out for particulate
168 matter (PM_{2.5}, PM₁₀), other trace gases (carbon monoxide (CO), O₃, nitric oxide (NO),
169 nitrogen dioxide (NO₂)), and meteorological data (Temperature, RH, WS, and wind
170 direction (WD)) based on 1 h resolution.

171 2.2 Positive Matrix Factorization (PMF) model

172 EPA PMF5.0 model was used for the quantitative source analysis of VOCs (Norris
173 et al., 2014). The principles and methods have been described in detail in previous
174 studies (Mozaffar et al., 2020; Zhang et al., 2021b). The decomposition of the PMF
175 mass balance equations is simplified as follows (Norris et al., 2014):

176

$$177 \quad x_{ij} = \sum_{k=1}^p g_{ik} f_{kj} + e_{ij} \quad (1)$$

178

179 where x_{ij} is the mass concentration of species j measured in sample i ; g_{ik} is the
180 contribution of factor k to the sample i ; f_{kj} represents the content of the j th species in
181 factor k ; e_{ij} is the residual of species j in sample i ; p represents the number of factors.
182 The fitting objective of the PMF model is to minimize the function Q to obtain the
183 factor contributions and contours. The formula for Q is given in Eq. (2):

184

$$185 \quad Q = \sum_{i=1}^n \sum_{j=1}^m \left[\frac{x_{ij} - \sum_{k=1}^p g_{ik} f_{kj}}{u_{ij}} \right]^2 \quad (2)$$

186

187 where n and m denote the number of samples and VOC species, respectively.

188 Concentrations and uncertainty data are required for the PMF model. In this study,

189 the median concentration of a given species is used to replace missing values with an
190 uncertainty of four times of the median values; data less than the Method Detection
191 Limit (MDL) were replaced with half the MDL, with an uncertainty of 5/6 of the MDL;
192 and the uncertainty for values greater than the MDL was calculated using Eq. (3). In
193 Eq. (3), EF is error fraction, expressed as the precision of VOCs species, and the setting
194 range can be adjusted from 5 to 20% according to the concentration difference (Buzcu
195 et al., 2006; Song et al., 2007); and c_{ij} is the concentration of species j in sample i :

$$196 \quad U_{ij} = \sqrt{(EF \times c_{ij})^2 + (0.5 \times MDL)^2} \quad (3)$$

197 when the concentration of VOCs in the species is less than the value of the
198 detection limit U_{ij} is calculated using Eq. (4):

$$199 \quad U_{ij} = \left(\frac{5}{6}\right) MDL \quad (4)$$

200 VOC species and concentration input into PMF were carefully selected to ensure
201 the accuracy of the PMF results. Species were excluded when over 25% of the samples
202 were missing or concentrations values were below the MDL (Gao et al., 2018); VOCs
203 with a short lifetime in the atmosphere were also excluded unless they are source-
204 relative species (Zhang et al., 2014; Shao et al., 2016). After that, retained VOC species
205 were categorized according to the signal-to-noise ratio (S/N) with $S/N < 0.2$ species
206 categorized as bad, $0.2 < S/N < 2$ species categorized as weak; and $S/N > 2$ species
207 categorized as strong (Shao et al., 2016).

208 We used displacement of factor elements (DISP) to assess PMF modelling
209 uncertainty (for a description, see Paatero et al. (2014)). Q was less than 1% and no
210 swaps occurred for the small est dQ^{\max} in DISP. F_{peak} values from -2 to 2 were tested
211 to explore the rotational stability of the solutions. $Q_{\text{true}}/Q_{\text{exp}}$ is lowest when $F_{\text{peak}} = 0$,
212 so we chose the PMF results for that case (Fig. S2a). After examining 3-8 factors, 20
213 base runs with 5 factors eventually selected to represent final result. We provide an
214 explanation of factor selection in the supplementary materials. Fig. S2(b) includes
215 $Q_{\text{true}}/Q_{\text{exp}}$, $Q_{\text{robust}}/Q_{\text{exp}}$ for factors 3-8. The slopes of these two ratios in changed at five
216 factors, and we found that five factors were more realistic after repeated comparisons
217 of the results at four, five and six factors.

218 2.3 SOA generation potential

219 The contributions of VOC species to SOAP were calculated based on the toluene
220 weighted mass contributions (TMC) method (Derwent et al., 2010). The methodology
221 for calculating SOAP is as follows:

$$222 \text{SOAPF}_i = \frac{\text{VOCs component } i \text{ to SOA mass concentration increments}}{\text{Toluene to SOA mass concentration increment}} \times 100 \quad (5)$$

224
225 SOAPF_i for each VOC is taken from the literature (Derwent et al., 2010). The
226 SOAP was estimated by multiplying the SOAPF_i value by the concentration of
227 individual VOC species. The SOAP calculations through each VOC are as follows:

$$228 \text{SOAP} = \sum E_i \times \text{SOAPF}_i \quad (6)$$

229 E_i is the concentration of species i .

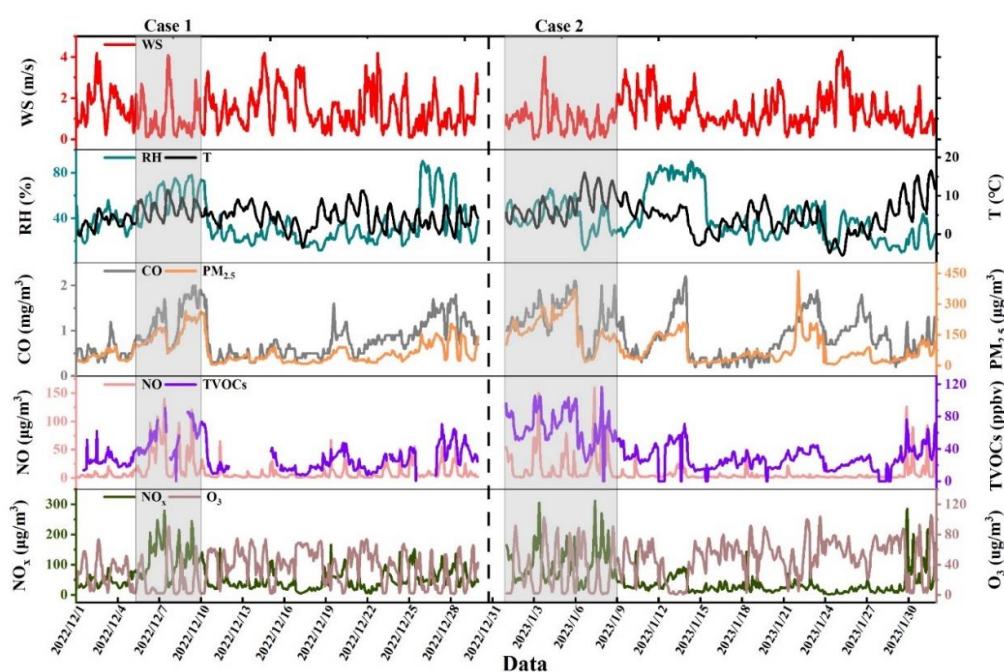
230 3. Results and discussion

231 3.1 Overview of variation in pollutants and meteorological 232 parameters

233 Figure 1 shows the time series of meteorological parameters, TVOCs, O₃, NO_x,
234 SO₂, CO and PM_{2.5} during the observed periods. Low WS and Temperature were found
235 with an average value of 1.3 ± 0.6 m/s and 5.0 ± 2.5 °C, respectively, during the entire
236 period, comparable with observations at the same site in 2021 (Lai et al., 2024). A total
237 of 62 days of valid data was acquired with the daily average concentration of PM_{2.5}
238 ranging from 53 to 239 $\mu\text{g}/\text{m}^3$, with the average value of 111 ± 45 $\mu\text{g}/\text{m}^3$. The
239 concentration of TVOCs ranged from 15.6 to 57.1 ppbv with an average of 36.1 ± 21.0
240 ppbv, higher than the same period in last year (27.9 ± 12.7 ppbv, Lai et al., 2024).
241 During the observation period, the average values of T, WS and RH were 5.0 ± 2.5 °C,
242 1.3 ± 0.6 m/s and $38.9 \pm 16.7\%$, respectively.

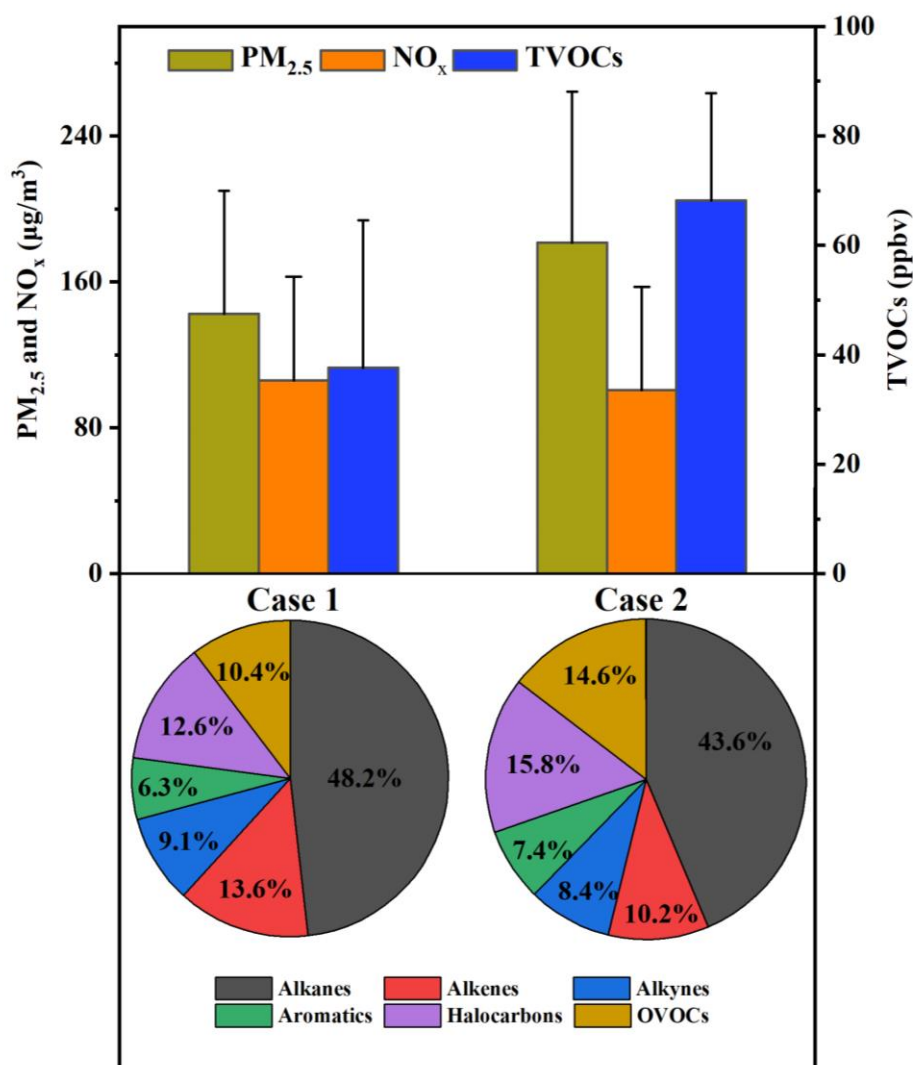
243 The relationship between meteorological parameters and pollutant concentrations
244 were analyzed and correlations between PM_{2.5}, TVOCs and NO_x and RH were found
245 (Fig. S3), suggesting that meteorological conditions have an important influence on
246 pollution formation. The comparisons of average concentrations of different periods

249 between different periods are presented in Tables 1 and 2. WS, Temp and RH
 250 conditions during infection and recovery periods were generally similar. However, the
 251 average concentration of PM_{2.5} during the recovery period was 1.6 times the value
 252 during the infection period. Furthermore, the concentrations of other pollutants
 253 including SO₂, NO₂, CO, and O₃ all showed a similar trend between infection and
 254 recovery periods. The TVOCs concentration during the recovery period was 1.2 times
 255 the value during the infection period, showing an obvious increase trend after
 256 resuming production. Decreased trends of air pollutants were found in other studies
 257 before and after the outbreak of the novel coronavirus (COVID-19) in early 2020 (Qi
 258 et al., 2021; Wang et al., 2021).



259
 260 Fig. 1. Time series of WS, T, RH, CO, PM_{2.5}, NO, TVOCs, NO_x and O₃ during the observation
 261 period.

262 The shadow section in Fig. 1 represents two haze pollution events during the
 263 monitoring period. A pollution event is determined when the daily average
 264 concentration of PM_{2.5} exceeds 75 µg/m³ (China's II-level standard) for at least three
 265 consecutive days. Case 1 (December 5 to December 10 with daily average PM_{2.5} =
 266 142.5 µg/m³) and Case 2 (January 1 to January 8 with daily average PM_{2.5} = 181.5
 267 µg/m³) were selected as they represent the pollution events in infection and
 268 recovery periods, respectively, due to their long duration and high pollution levels. Any days with
 269 a PM_{2.5} concentration lower than 35 µg/m³ (China's I-level standard) is considered as
 270 Clean days.



271

272 Fig. 2. The concentration of PM_{2.5}, NO_x, TVOCs and the composition ratio of VOCs in Case 1 and
 273 Case 2.

274 As for the two representative pollution processes (Case 1 during the infection
 275 period and Case 2 during the recovery period), the concentration of TVOCs in Case 1
 276 and Case 2 were 48.4 ± 20.4 and 67.6 ± 19.6 ppbv (Fig. 2), respectively, increased by
 277 63% and 188% compared with values during clean days. The average concentrations
 278 of PM_{2.5} and TVOCs during Case 2 were 1.3 and 1.8 times the values in Case 1. The
 279 highest volume contributions of alkanes were found both in Case 1 (48%) and Case 2
 280 (44%), consistent with the results in the Yangtze River Delta region (36-43%, Liu et al.,
 281 2023). While alkenes exhibited higher volume percentages of 13% in Case 1, followed
 282 by halogenated hydrocarbon (12%) and OVOCs (10%). Higher volume percentages of
 283 alkanes and alkenes in Case 1 were similar to the results in the gasoline evaporation
 284 site in winter (Niu et al., 2022). Equivalent volume contribution of halogenated
 285 hydrocarbon and OVOCs (15%) were found in Case 2, followed by alkenes (10%).

286 Though the volume contributions of aromatics were the lowest (6% in Case 1 and 7%
 287 in Case 2), the highest increase ratio was found from clean days to polluted episodes.

288 Table 1 The average concentrations of meteorological parameters and pollutants during different
 289 processes.

Category	Entire process	Infection period	Recovery period	Case 1	Case 2
	N = 62 days	N = 31 days	N = 31 days	N = 6 days	N = 8 days
WS (m/s)	1.3 ± 0.6	1.4 ± 0.6	1.3 ± 0.6	1.2 ± 0.9	0.9 ± 0.7
T (°C)	5.0 ± 2.5	4.7 ± 1.7	5.4 ± 3.1	6.1 ± 2.2	7.4 ± 3.5
RH (%)	38.9 ± 16.7	37.6 ± 15.5	40.2 ± 18.2	55.7 ± 14.7	42.0 ± 12.1
TVOCs (ppbv)	36.1 ± 21.0	31.9 ± 18.1	39.8 ± 22.4	37.6 ± 27.0	68.2 ± 19.6
SO ₂ (µg/m ³)	11.4 ± 2.7	10.2 ± 2.8	12.7 ± 2.3	11.0 ± 3.7	16.2 ± 6.1
NO ₂ (µg/m ³)	47.2 ± 10.0	46.8 ± 8.6	47.8 ± 11.7	62.7 ± 20.5	65.0 ± 21.3
CO (mg/m ³)	0.9 ± 0.2	0.8 ± 0.2	1.1 ± 0.2	1.2 ± 0.5	1.3 ± 0.4
O ₃ (µg/m ³)	34.9 ± 6.0	31.1 ± 4.5	39.0 ± 4.6	21.8 ± 23.7	32.5 ± 29.6
PM _{2.5} (µg/m ³)	111.5 ± 45.1	86.6 ± 34.6	138.3 ± 39.6	142.5 ± 67.4	181.5 ± 82.7

290 Table 2 Concentration of VOC species during different processes (ppbv).

Category	Entire process	Infection period	Recovery period	Case 1	Case 2	Clean days
TVOCs	36.1 ± 21.0	31.9 ± 18.1	39.8 ± 22.4	48.4 ± 20.4	67.6 ± 19.6	17.5 ± 9.5
alkanes	16.8 ± 9.2	15.0 ± 8.4	18.4 ± 9.5	23.1 ± 10.0	29.5 ± 8.4	9.2 ± 5.6
alkenes	4.1 ± 2.7	3.8 ± 2.6	4.4 ± 2.7	6.5 ± 2.9	7.0 ± 2.6	1.7 ± 1.3
alkynes	3.1 ± 2.0	2.7 ± 1.7	3.4 ± 2.1	4.3 ± 2.0	5.8 ± 1.9	1.3 ± 0.8
aromatics	2.1 ± 2.0	1.8 ± 1.5	2.3 ± 2.2	3.0 ± 1.8	4.9 ± 2.8	0.7 ± 0.5
halogenated hydrocarbon	5.4 ± 3.3	4.4 ± 2.3	6.2 ± 3.8	6.0 ± 1.9	10.7 ± 3.6	2.7 ± 1.4
OVOCs	4.6 ± 3.2	3.5 ± 2.7	5.1 ± 3.5	5.0 ± 2.4	9.7 ± 2.8	1.9 ± 1.1

291 3.2 Source Analysis of VOCs

292 Specific VOC ratios can be used for initial source identification of VOCs and
 293 determination of photochemical ages of air masses (Monod et al., 2001; An et al., 2014;
 294 Li et al., 2019). In this study, the ratios of toluene/benzene (T/B), isopentane/n-pentane,
 295 isobutane/n-butane, and m/p-xylene/ethylbenzene (X/E) were selected to initially
 296 identify the potential sources of VOCs (Fig. 3). Concentrations of selected pollutants
 297 and ratios used are shown in Table S1.

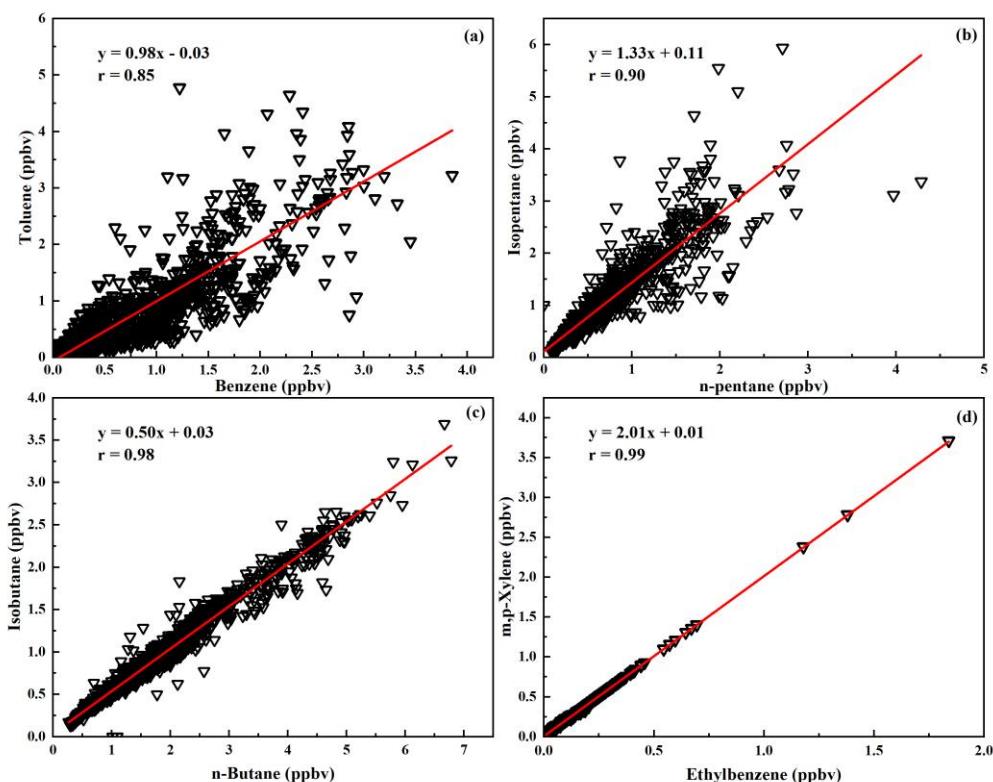
298 Toluene-to-benzene ratio (T/B ratio) was widely used to assess the relative

299 importance of different sources. Specifically, T/B ratio with the value of 1.3–3.0 was
300 observed in vehicle emissions for vehicles with different fuel types (Schauer et al., 2002;
301 Wang et al., 2015). The reported T/B ratio for combustion processes was between 0.13
302 and 0.7 (Li et al., 2011; Wang et al., 2014). The average T/B value for the entire period
303 was 1.0, indicating that both traffic emissions and combustion are significant sources
304 of VOCs.

305 The isopentane/n-pentane concentration ratios of 0.6-0.8 represent mainly coal
306 combustion emissions, ratios of 0.8-0.9 represent liquefied petroleum gas (LPG)
307 emissions, 2.2-3.8 represent vehicle exhaust emissions, and 1.8-4.6 represent fuel
308 evaporation (Conner et al., 1995; Liu et al., 2008; Li et al., 2019). The overall ratio of
309 isopentane/n-pentane is 1.4, indicating that pentane is mainly derived from the
310 combined effects of liquid petrol and fuel evaporation.

311 Isobutane/n-butane concentration ratios of 0.2-0.3 represent vehicle emissions,
312 0.4-0.6 represent LPG usage, and 0.6-1.0 represent natural gas emissions (Russo et al.,
313 2010; Zheng et al., 2018). The ratio of isobutane/n-butane in this study was 0.50, which
314 suggests that the VOC concentrations at the observation sites are influenced by natural
315 gas emissions (Shao et al., 2016; Zeng et al., 2023).

316 The ratio of X/E can be used to infer the photochemical age of the air mass. X/E
317 ratios around 2.5-2.9 are typical of urban areas, indicating that VOCs are mainly from
318 the urban area (fresh air mass) (Kumar et al., 2018). When this ratio is significantly
319 lower than 3, it indicates that VOCs are mainly transported from distant sources (aging
320 air masses) (Kumar et al., 2018). The average X/E value in this study was 2.0 (Fig.
321 3(d)), indicating low photochemical activity and aging of the air mass at the observation
322 site. Potential source analyses also indicate that air masses are affected by long-range
323 transport (Fig. S4).



324

325

Fig. 3. Correlation analysis between specific VOC species.

326

Figure 4 shows the chemical profiles of individual VOCs resolved by the PMF model during the entire observation period. These five factors eventually selected as potential sources for the observed VOCs are: (1) Fuel evaporation; (2) Solvent usage; (3) Vehicular emission; (4) Industrial source; and (5) Combustion. These 5 factors have been commonly reported before, e.g., in Shijiazhuang, northern China (Guan et al, 2023) and in Beijing (Cui et al., 2022).

332

Alkanes of C4-C6 substances were predominant in factor 1, including 2-methylpentane, 3-methylpentane, isobutane, n-butane, isopentane and n-pentane from oil and gas (Xiong et al., 2020). Fig. S5 shows that emissions from this source peak at midday, when fuel volatilization is high, The CPF plot shows that south-east is the dominant direction at wind speeds of less than 2 m/s (Fig. 5a). Therefore, factor 1 was identified as the source of oil and gas volatilization.

338

The contribution of benzene, toluene, methylene chloride, 1,2-dichloroethane and ethyl acetate was high in factor 2. It has been shown that benzene, toluene, ethylbenzene, and xylene is an important component in the use of solvents (Li et al., 2015); methylene chloride is often used as a chemical solvent, while esters are mostly used as industrial solvents or adhesives (Li et al., 2015). Factor 2 is determined to be solvent usage source.

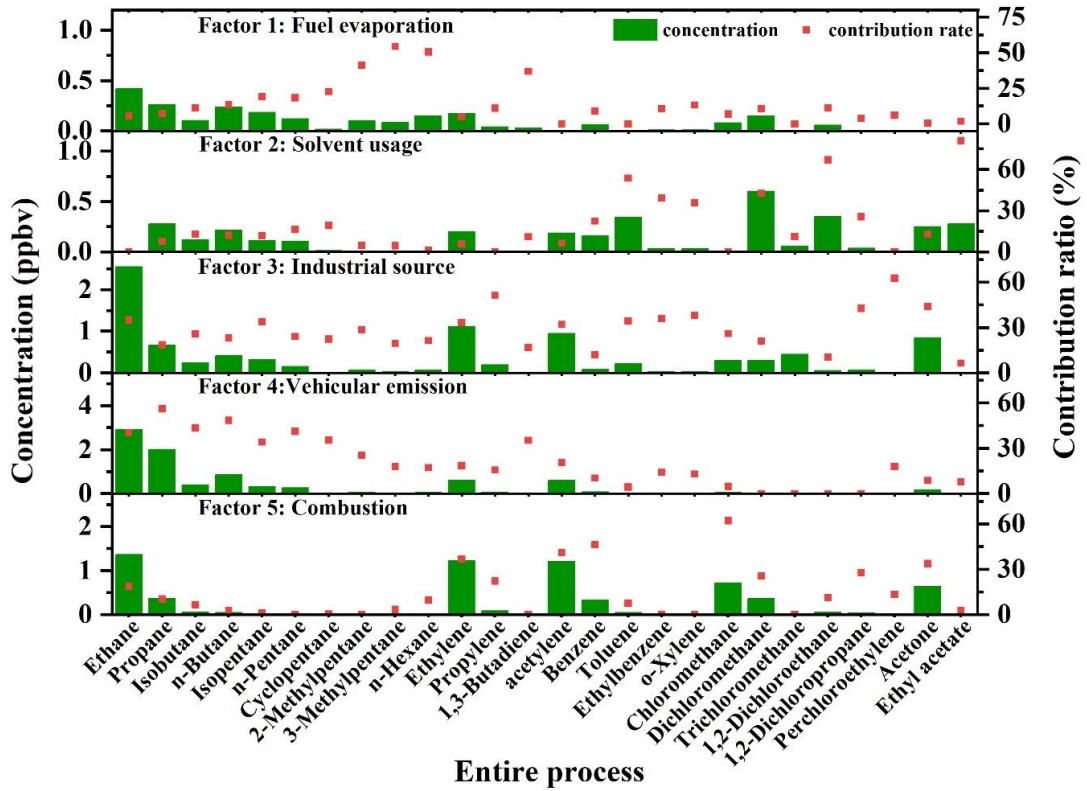
342

343 The CPF plot shows that local sources with wind speeds less than 1 m/s are the main
344 sources (Fig. 5b).

345 Factor 3 contains predominantly C3-C8 alkanes, olefins and alkynes, and
346 relatively high concentrations of benzene. These substances are usually emitted by
347 industrial processes (Shao et al., 2016), so Factor 4 is defined as an industrial source.
348 The CPF plots indicate that a local source at low wind speeds is the dominant sources
349 (Fig. 5c).

350 Factor 4 is characterized by relatively high levels of C2-C6 low-carbon alkanes
351 (ethane, propane, isopentane, n-pentane, isobutane and n-butane), olefins (ethylene and
352 propylene), and benzene and toluene, which are important automotive exhaust tracers
353 (Song et al., 2021; Zhang et al., 2021b). Ethylene and propylene are important
354 components derived from vehicle-related activities. Previous studies of VOCs in
355 Zhengzhou have shown a high percentage of VOCs emitted from gasoline vehicles,
356 with the main source of alkanes being on-road mobile sources (Bai et al., 2020). The
357 daily variation of this source in Fig. S5 shows a bimodal trend, with peaks occurring in
358 the morning and evening peaks of traffic, consistent with motor vehicle emissions. Fig.
359 5d shows that this source is mainly from the west where wind speeds are below 2 m/s,
360 and in this direction, there are a number of urban arterial roads with high traffic volumes.
361 Therefore, factor 4 was defined as vehicular emission source.

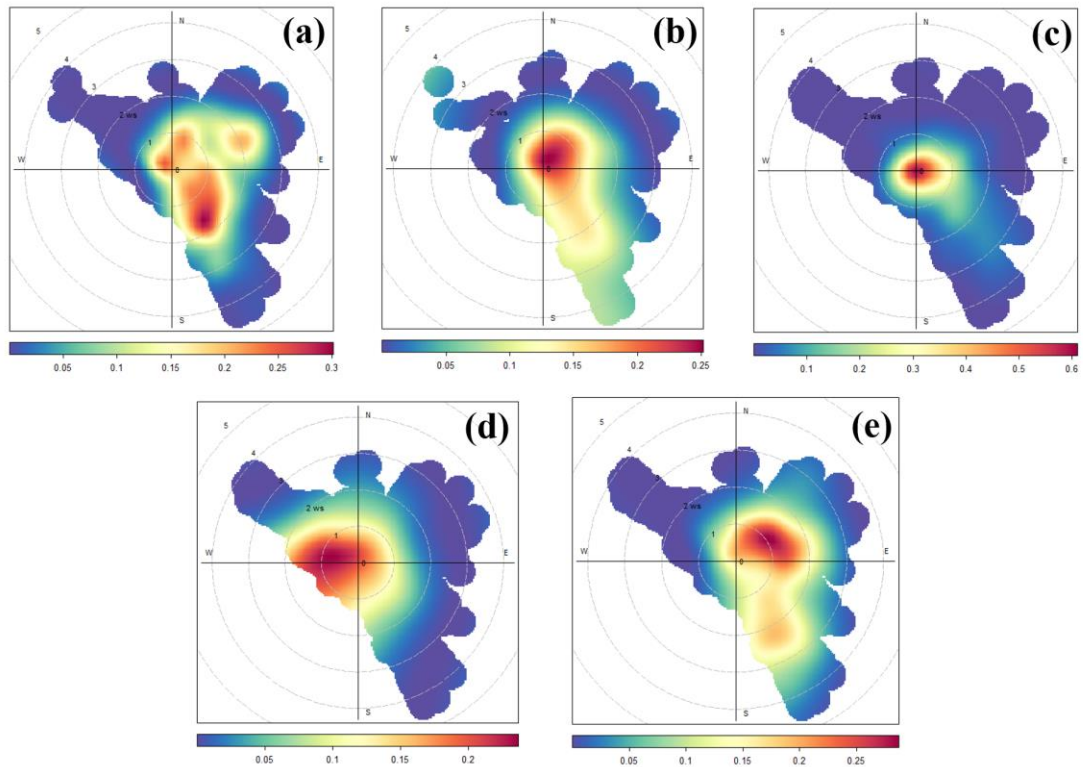
362 The highest contribution to factor 5 is chloromethane (62%). Benzene (46%) and
363 acetylene (41%) also contribute highly to factor 5. Chloromethane is the key tracer for
364 biomass combustion and acetylene is the key tracer for coal combustion (Xiong et al.,
365 2020). Therefore, factor 5 is defined as a combustion source. The CPF plot shows that
366 at wind speeds below 2 m/s, the north-east direction is the dominant source direction
367 (Fig. 5e).



368

369

Fig. 4. Concentration of VOC species in each factor and contribution to each source.



370

371

372

Note: a: Fuel evaporation; b: Solvent usage; c: Industrial source; d: Vehicular emission; e: Combustion.

373

Fig. 5. CPF plots of five VOCs sources obtained using the PMF model.

374

375

376

377

378

379

380

381

382

383

Figure S6 compares the differences in PMF factor/source profiles during the peak of Omicron infection with those during the recovery phase after the peak, as well as between contaminated and clean days. We present the concentrations of the five main VOCs in all five factors in Table S2. Ethane (vehicular emission), 2-methylpentane (fuel evaporation), benzene (industry source), chloromethane (combustion), and ethyl acetate (solvent usage) were selected as tracers for five sources. Ethane concentration in Case 2 (5.9 ppbv) is much higher than in other processes, and ethane concentration during the recovery period (3.4 ppbv) is also higher than during the infection period (2.4 ppbv), which may to some extent reflect increased vehicular emissions during the recovery period.

384

385

386

387

388

389

390

391

392

393

394

Concentrations of most species were significantly higher during the recovery period than during the infection period. The representative pollution processes in both periods showed the same results as well, with a 79% higher concentration of TVOCs in Case 2 (65.1 ppbv) compared to Case 1 (36.3 ppbv) (Fig. 6). While in Case 1 industry was the dominant source of VOCs, by Case 2 motorized sources reached a concentration value of 21.2 ppbv, accounting for 33% of the observed VOCs, and became the dominant source of emissions. This is consistent with the fact that people's mobility activities have increased after the epidemic has entered the recovery period. As a group of VOCs species with the highest concentration share, ethane and propane contributed more to the clean days motor vehicle source than other processes, which also resulted in a 34% clean days motor vehicle source share.

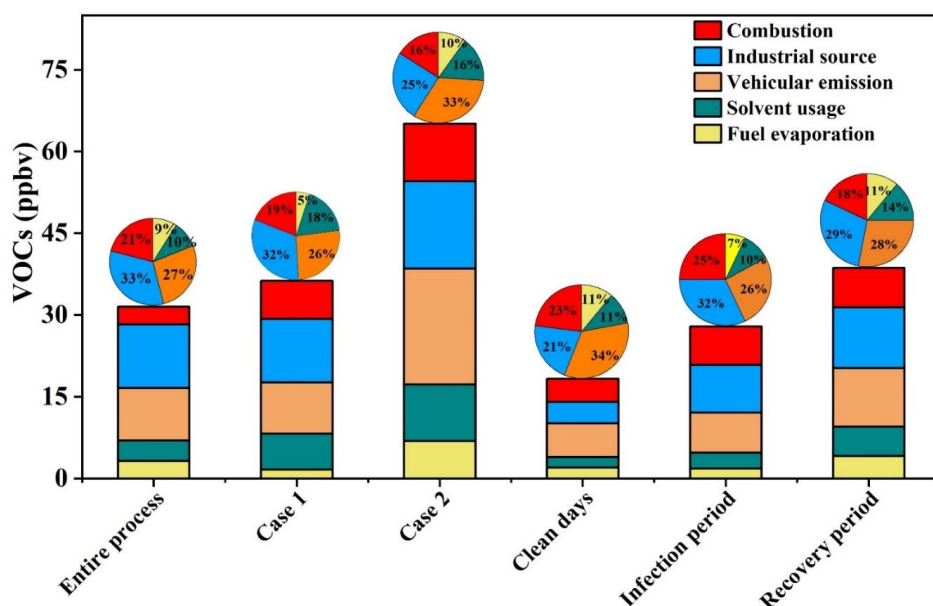


Fig. 6. Contribution of each to VOCs for different processes.

3.3 SOAP

VOCs are estimated to contribute about 16–30% or more of $PM_{2.5}$ by mass through SOA production (Huang et al., 2014). Therefore, by calculating the SOAP value, the influence of different sources on $PM_{2.5}$ production can be reflected to a certain extent.

We have included quantitative analysis for SOAP as well. Fig. 7 shows the SOAP concentrations and contribution rates of the top ten species throughout the entire process, during two pollution processes, and clean days. The top ten species all reached close to 100% of the total SOAP contribution, with Case 1 reaching 98%. In each process, the composition of the top ten substances is essentially the same. Aromatic hydrocarbons contributed the most, with BTEX always occupying the top five positions and toluene the most. The SOAP values of the top ten contributing species for the two polluting processes are shown in Tables S3 and S4. Toluene, the highest contributing species, reached a SOAP value of $49.4 \mu\text{g}/\text{m}^3$ in the most polluted Case 2, which was 3.2 times higher than the SOAP sum of all species on the clean day ($15.5 \mu\text{g}/\text{m}^3$). The SOAP value for Case 1, which is also a contaminated process, was $67 \mu\text{g}/\text{m}^3$, and the main species (m/xylene: $9.8 \mu\text{g}/\text{m}^3$, benzene: $8.5 \mu\text{g}/\text{m}^3$) including toluene ($34.6 \mu\text{g}/\text{m}^3$) were lower than those for Case 2 (m/xylene: $19.4 \mu\text{g}/\text{m}^3$, benzene: $13.4 \mu\text{g}/\text{m}^3$).

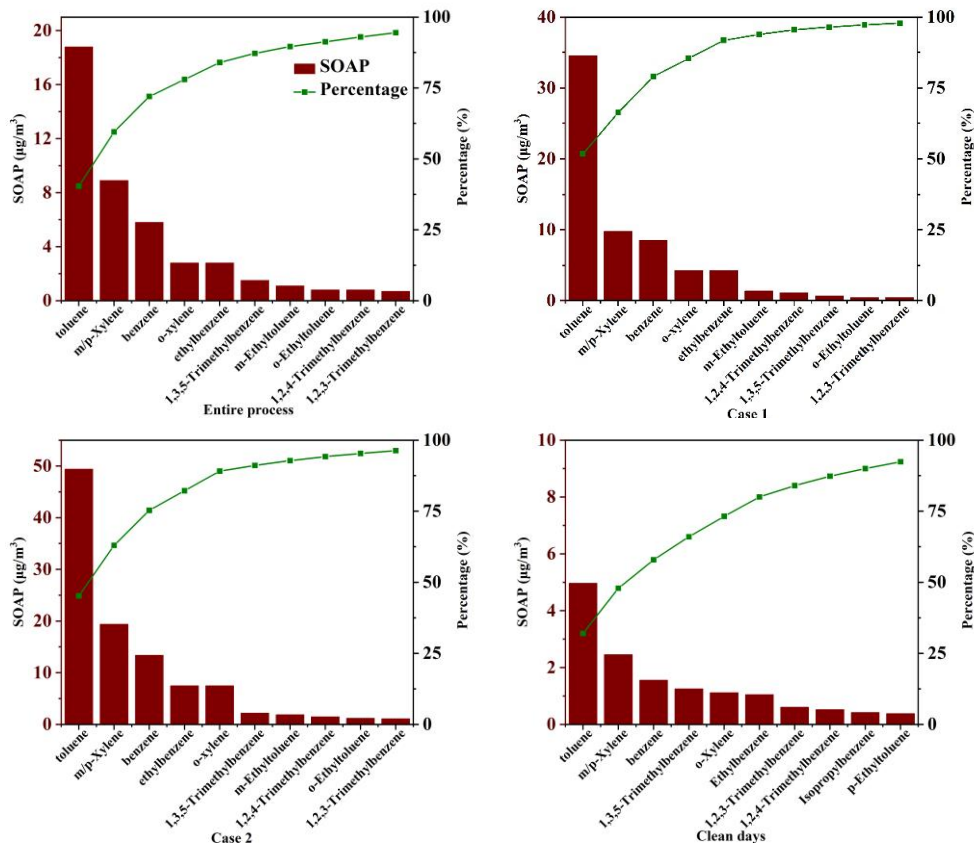


Fig. 7. SOAP dominant species in different processes

414
415
416
417
418
419
420
421
422
423
424
425
426
427

Figure 8 shows the SOAP calculated after source resolution of the two pollution processes by PMF for clean days, respectively. In Case 1, industrial source is the dominant source with a contribution ratio of 63%. In Case 2, the pollution sources exhibit a more evenly distributed contribution, where the solvent usage and fuel evaporation sources emerge as the primary contributors to SOAP, with their respective contribution levels rising to 32% and 26%. The clean day result with a SOAP of 8.8 µg/m³ also indicates that industrial and solvent usage sources are the most dominant SOAP sources. The primary sources of aromatic compounds, which are the most significant contributors to SOAP, are solvent usage and industrial process emissions. This finding aligns with the results of other studies (Wu et al., 2017). Consequently, it is imperative to implement measures to reduce PM_{2.5} pollution by regulating emissions from industrial and solvent usage sources.

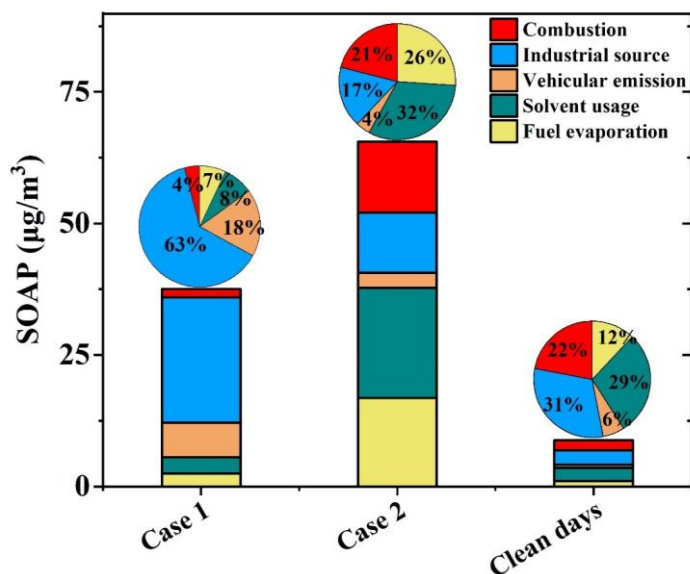


Fig. 8. SOAP value and contribution ratio of each process

428

429

430

431 4. Conclusions

432 Continuous observation of VOCs during the infection of the Omicron epidemic
 433 was carried out at an urban site in polluted Zhengzhou from December 1, 2022, to
 434 January 31, 2023. The daily average concentration of PM_{2.5} ranged from 53.5 to 239.4
 435 µg/m³ with an average value of 111.5 ± 45.1 µg/m³ during the whole period. The
 436 concentration of TVOCs ranged from 15.6 to 57.1 ppbv with an average of 36.1 ± 21.0
 437 ppbv, higher than the same period in last year (27.9 ± 12.7 ppbv, Lai et al., 2024).

438 Two representative contamination processes were identified (Case 1 during the
 439 infection period and Case 2 during the recovery period). The concentration of TVOCs
 440 in Case 1 and Case 2 were 48.4 ± 20.4 and 67.6 ± 19.6 ppbv, respectively, increased by
 441 63% and 188% compared with values during clean days. The average concentrations
 442 of PM_{2.5} and TVOCs during Case 2 were 1.3 and 1.8 times of the values in Case 1. The
 443 highest volume contributions of alkanes were found both in Case 1 (48%) and Case 2
 444 (44%). Though the volume contribution of aromatics were the lowest (6% in Case 1
 445 and 7% in Case 2), the highest increase ratio was found from clean days to polluted
 446 episodes.

447 Local sources were initially identified through T/B, isopentane/n-pentane,
 448 isobutane/n-butane, and X/E ratios. The average X/E value was 2.0, indicating that
 449 measured levels of airborne VOCs were influenced by emissions from remote sources
 450 and urban areas. The PMF receptor modeling yielded five major sources of pollution,
 451 which included industrial emissions (32%), vehicular emissions (27%), combustion

452 (21%), solvent usage (11%), and fuel evaporation (9%). Significant differences were
453 observed in the sources of VOCs across different pollution periods. In Case 1, industrial
454 emissions constituted the largest contributor, accounting for 32% of the total VOCs. In
455 contrast, in Case 2, the proportion of vehicular emissions increased to 33%, becoming
456 the primary source of VOCs.

457 Aromatic compounds are the main contributors to SOAP, with BTEX being the
458 main contributor during the entire period. SOAP values reached 37.6 and 65.6 $\mu\text{g}/\text{m}^3$,
459 respectively in Case 1 and Case 2. In Case 1, industrial source accounted for a
460 substantial majority (63%, 23.8 $\mu\text{g}/\text{m}^3$), while vehicular source, as the second most
461 significant contributor, made up only 18%. In Case 2, the distribution of contribution
462 rates was more uniform, with solvent usage source and fuel evaporation source
463 becoming the primary contributors to SOAP, at 32% (20.9 $\mu\text{g}/\text{m}^3$) and 26% (16.8 $\mu\text{g}/\text{m}^3$),
464 respectively. The SOAP result for the Clean Day was 8.8 $\mu\text{g}/\text{m}^3$, with industrial source
465 and solvent usage remaining the primary contributors. Consequently, it is of paramount
466 importance to regulate emissions from the industrial and solvent usage sectors with the
467 objective of reducing PM_{2.5} pollution.

468 **Acknowledgments:**

469 This research was supported by the Natural Science Foundation of Henan Province
470 (232300421395) and the National Key Research and Development Program of China
471 (2017YFC0212400).

472 **References**

473 An, J., Zhu, B., Wang, H., Li, Y., Lin, X., and Yang, H.: Characteristics and source
474 apportionment of VOCs measured in an industrial area of Nanjing, Yangtze River Delta,
475 China, Atmospheric Environment, 97, 206-214,
476 <https://doi.org/10.1016/j.atmosenv.2014.08.021>, 2014.

477 Bai, L., Lu, X., Yin, S., Zhang, H., Ma, S., Wang, C., Li, Y., and Zhang, R.: A
478 recent emission inventory of multiple air pollutant, PM_{2.5} chemical species and its
479 spatial-temporal characteristics in central China, Journal of Cleaner Production, 269,
480 122114, <https://doi.org/10.1016/j.jclepro.2020.122114>, 2020.

481 Buzcu, B. and Fraser, M. P.: Source identification and apportionment of volatile
482 organic compounds in Houston, TX, Atmospheric Environment, 40, 2385-2400,
483 <https://doi.org/10.1016/j.atmosenv.2005.12.020>, 2006.

484 Conner, T. L., Lonneman, W. A., Seila, R.L.: Transportation-related volatile
485 hydrocarbon source profiles measured in atlanta, *Journal of the Air & Waste*
486 *Management Association*, 45 (5), 383-394,
487 <https://doi.org/10.1080/10473289.1995.10467370>, 1995.

488 Cui, L., Wu, D., Wang, S., Xu, Q., Hu, R., and Hao, J.: Measurement report:
489 Ambient volatile organic compound (VOC) pollution in urban Beijing: characteristics,
490 sources, and implications for pollution control, *Atmospheric Chemistry and Physics*,
491 22, 11931-11944, <https://doi.org/10.5194/acp-22-11931-2022>, 2022.

492 Derwent, R. G., Jenkin, M. E., Utembe, S. R., Shallcross, D. E., Murrells, T. P.,
493 and Passant, N. R.: Secondary organic aerosol formation from a large number of
494 reactive man-made organic compounds, *Science of the Total Environment*, 408, 3374-
495 3381, <https://doi.org/10.1016/j.scitotenv.2010.04.013>, 2010.

496 Gao, J., Zhang, J., Li, H., Li, L., Xu, L., Zhang, Y., Wang, Z., Wang, X., Zhang,
497 W., Chen, Y., Cheng, X., Zhang, H., Peng, L., Chai, F., and Wei, Y.: Comparative study
498 of volatile organic compounds in ambient air using observed mixing ratios and initial
499 mixing ratios taking chemical loss into account – A case study in a typical urban area
500 in Beijing, *Science of the Total Environment*, 628-629, 791-804,
501 <https://doi.org/10.1016/j.scitotenv.2018.01.175>, 2018.

502 Guan, Y., Liu, X., Zheng, Z., Dai, Y., Du, G., Han, J., Hou, L. a., and Duan, E.:
503 Summer O₃ pollution cycle characteristics and VOCs sources in a central city of
504 Beijing-Tianjin-Hebei area, China, *Environmental Pollution*, 323, 121293,
505 <https://doi.org/10.1016/j.envpol.2023.121293>, 2023.

506 Huang, R., Zhang, Y., Bozzetti, C. et al.: High secondary aerosol contribution to p
507 articulate pollution during haze events in China, *Nature*, 514 (7521), 218–22, <https://doi.org/10.1038/nature13774>, 2014.

509 Hui, L., Liu, X., Tan, Q., Feng, M., An, J., Qu, Y., Zhang, Y., Deng, Y., Zhai, R., a
510 nd Wang, Z.: VOC characteristics, chemical reactivity and sources in urban Wuhan, ce
511 ntral China, *Atmospheric Environment*, 224, 117340, <https://doi.org/10.1016/j.atmosenv.2020.117340>, 2020.

513 Jensen, A., Liu, Z., Tan, W., Dix, B., Chen, T., Koss, A., Zhu, L., Li, L., de Gouw,
514 J.: Measurements of volatile organic compounds during the COVID-19 lockdown in
515 Changzhou, China, *Geophysical research letters*, 48(20), <https://doi.org/10.1029/2021GL095560>, 2021.

517 Jiang, N., Hao, X., Hao, Q., Wei, Y., Zhang, Y., Lyu, Z., Zhang, R.: Changes in se

518 condary inorganic ions in PM_{2.5} at different pollution stages before and after COVID-1
519 9 control, *Environmental Science*, 44(5), 2430-2440, [https://doi.org/10.13227/j.hjxk.2](https://doi.org/10.13227/j.hjxk.202206170)
520 [02206170](https://doi.org/10.13227/j.hjxk.202206170), 2023.

521 Kumar, A., Singh, D., Kumar, K., Singh, B. B., and Jain, V. K.: Distribution of
522 VOCs in urban and rural atmospheres of subtropical India: Temporal variation, source
523 attribution, ratios, OFP and risk assessment, *Science of the Total Environment*, 613-614,
524 492-501, <https://doi.org/10.1016/j.scitotenv.2017.09.096>, 2018.

525 Lai, M., Zhang, D., Yin, S., Song, X., and Zhang, R.: Pollution characteristics,
526 source apportionment and activity analysis of atmospheric VOCs during winter and
527 summer pollution in Zhengzhou City, *Environmental Science*, 4108, 3500-3510,
528 <https://doi.org/10.13227/j.hjxk.202001133>, 2024.

529 Li, B., Ho, S. S. H., Gong, S., Ni, J., Li, H., Han, L., Yang, Y., Qi, Y., and Zhao,
530 D.: Characterization of VOCs and their related atmospheric processes in a central
531 Chinese city during severe ozone pollution periods, *Atmospheric Chemistry and*
532 *Physics*, 19, 617-638, <https://doi.org/10.5194/acp-19-617-2019>, 2019.

533 Li, J., Deng, S., Tohti, A., Li, G., Yi, X., Lu, Z., Liu, J., and Zhang, S.: Spatial
534 characteristics of VOCs and their ozone and secondary organic aerosol formation
535 potentials in autumn and winter in the Guanzhong Plain, China, *Environmental*
536 *Research*, 211, 113036, <https://doi.org/10.1016/j.envres.2022.113036>, 2022.

537 Li, J., Xie, S. D., Zeng, L. M., Li, L. Y., Li, Y. Q., and Wu, R. R.: Characterization
538 of ambient volatile organic compounds and their sources in Beijing, before, during, and
539 after Asia-Pacific Economic Cooperation China 2014, *Atmospheric Chemistry and*
540 *Physics*, 15, 7945-7959, <https://doi.org/10.5194/acp-15-7945-2015>, 2015.

541 Li, J., Lu, K., Lv, W., Li, J., Zhong, L., Ou, Y., Chen, D., Huang, X., and Zhang,
542 Y.: Fast increasing of surface ozone concentrations in Pearl River Delta characterized
543 by a regional air quality monitoring network during 2006–2011, *Journal of*
544 *Environmental Sciences*, 26, 23-36, [https://doi.org/10.1016/S1001-0742\(13\)60377-0](https://doi.org/10.1016/S1001-0742(13)60377-0),
545 2014.

546 Liu, Y., Li, X., Tang, G., Wang, L., Lv, B., Guo, X., and Wang, Y.: Secondary
547 organic aerosols in Jinan, an urban site in North China: Significant anthropogenic
548 contributions to heavy pollution, *Journal of Environmental Sciences*, 80, 107-115,
549 <https://doi.org/10.1016/j.jes.2018.11.009>, 2019.

550 Liu, Y., Shao, M., Fu, L., Lu, S., Zeng, L., and Tang, D.: Source profiles of volatile
551 organic compounds (VOCs) measured in China: Part I, *Atmospheric Environment*, 42,

552 6247-6260, <https://doi.org/10.1016/j.atmosenv.2008.01.070>, 2008.

553 Liu, Y., Song, M., Liu, X., Zhang, Y., Hui, L., Kong, L., Zhang, Y., Zhang, C., Qu,
554 Y., An, J., Ma, D., Tan, Q., and Feng, M.: Characterization and sources of volatile
555 organic compounds (VOCs) and their related changes during ozone pollution days in
556 2016 in Beijing, China, *Environmental Pollution*, 257, 113599,
557 <https://doi.org/10.1016/j.envpol.2019.113599>, 2020.

558 Liu, Z., Hu, K., Zhang, K., Zhu, S., Wang, M., and Li, L.: VOCs sources and roles
559 in O₃ formation in the central Yangtze River Delta region of China, *Atmospheric*
560 *Environment*, 302, <https://doi.org/10.1016/j.atmosenv.2023.119755>, 2023.

561 Li, X., Wang, S., Hao, J.: Characteristics of volatile organic compounds (VOCs)
562 emitted from biofuel combustion in China, *Environmental Science*, 32, 3515-3521,
563 2011.

564 Li, Y., Yin, S., Zhang R., Yu, S., Yang, J., and Zhang, D.: Characteristics and source
565 apportionment of atmospheric VOCs at different pollution levels in winter in an urban
566 area in Zhengzhou, *Environmental Science*, 4108, 3500-3510,
567 <https://doi.org/10.13227/j.hjcx.202001133>, 2020.

568 Ma, Q., Wang, W., Wu, Y., Wang, F., Jin, L., Song, Y., Han, Y., Zhang, R., Zhang,
569 D.: Haze caused by NO_x oxidation under restricted residential and industrial activities
570 in a mega city in the south of North China Plain, *Chemosphere*, Volume 305, 135489,
571 <https://doi.org/10.1016/j.chemosphere.2022.135489>, 2022.

572 Merino, M., Marinescu, M., Cascajo, A., Carretero, J., Singh, D.: Evaluating the
573 spread of Omicron COVID-19 variant in Spain, *Future Generation Computer Systems*,
574 149, 547-561, <https://doi.org/10.1016/j.future.2023.07.025>, 2023.

575 Monod, A., Sive, B. C., Avino, P., Chen, T., Blake, D. R., and Sherwood Rowland,
576 F.: Monoaromatic compounds in ambient air of various cities: a focus on correlations
577 between the xylenes and ethylbenzene, *Atmospheric Environment*, 35, 135-149,
578 [https://doi.org/10.1016/S1352-2310\(00\)00274-0](https://doi.org/10.1016/S1352-2310(00)00274-0), 2001.

579 Mozaffar, A., Zhang, Y.-L., Fan, M., Cao, F., and Lin, Y.-C.: Characteristics of
580 summertime ambient VOCs and their contributions to O₃ and SOA formation in a
581 suburban area of Nanjing, China, *Atmospheric Research*, 240, 104923,
582 <https://doi.org/10.1016/j.atmosres.2020.104923>, 2020.

583 Mu, L., Feng, C., Li, Y., Li, X., Liu, T., Jiang, X., Liu, Z., Bai, H., and Liu, X.:
584 Emission factors and source profiles of VOCs emitted from coke production in Shanxi,
585 China, *Environmental Pollution*, 335, 122373,

586 <https://doi.org/10.1016/j.envpol.2023.122373>, 2023.

587 Niu, Y., Yan, Y., Chai, J., Zhang, X., Xu, Y., Duan, X., Wu, J., and Peng, L.: Effects
588 of regional transport from different potential pollution areas on volatile organic
589 compounds (VOCs) in Northern Beijing during non-heating and heating periods,
590 *Science of the Total Environment*, 836, 155465,
591 <https://doi.org/10.1016/j.scitotenv.2022.155465>, 2022.

592 Norris, G., Duvall, R., Brown, S., Bai, S. EPA Positive Matrix Factorization (PMF)
593 5.0 Fundamentals and User Guide. U.S. Environmental Protection Agency, Washington,
594 DC, EPA/600/R-14/108 (NTIS PB2015-105147), 2014.

595 Paatero, P., Eberly, S., Brown, S. G., Norris, G. A.: *Methods for estimating*
596 *uncertainty in factor analytic solutions*, *Atmospheric Measurement Techniques*, Volume
597 7, 781-797, <https://doi.org/10.5194/amt-7-781-2014>, 2014.

598 Pei, C., Yang, W., Zhang, Y., Song, W., Xiao, S., Wang, J., Zhang, J., Zhang, T.,
599 Chen, D., Wang, Y., Chen, Y., Wang, X.: *Decrease in ambient volatile organic*
600 *compounds during the COVID-19 lockdown period in the Pearl River Delta region,*
601 *south China*, *Science of The Total Environment*, 823, 153720,
602 <https://doi.org/10.1016/j.scitotenv.2022.153720>, 2022.

603 Petersen, M. S., Í Kongsstovu, S., Eliassen, E. H., Larsen, S., Hansen, J. L., Vest,
604 N., Dahl, M. M., Christiansen, D. H., Møller, L. F., & Kristiansen, M. F.: *Clinical*
605 *characteristics of the Omicron variant - results from a Nationwide Symptoms Survey*
606 *in the Faroe Islands*, *International Journal of Infectious Diseases*, 122, 636–643,
607 <https://doi.org/10.1016/j.ijid.2022.07.005>, 2022.

608 Qi, J., Mo, Z., Yuan, B., Huang, S., Huangfu, Y., Wang, Z., Li, X., Yang, S., Wang,
609 W., Zhao, Y., Wang, X., Wang, W., Liu, K., and Shao, M.: *An observation approach in*
610 *evaluation of ozone production to precursor changes during the COVID-19 lockdown,*
611 *Atmospheric Environment*, 262, 118618,
612 <https://doi.org/10.1016/j.atmosenv.2021.118618>, 2021.

613 Russo, R. S., Zhou, Y., White, M. L., Mao, H., Talbot, R., and Sive, B. C.: *Multi-*
614 *year (2004–2008) record of nonmethane hydrocarbons and halocarbons in New*
615 *England: seasonal variations and regional sources*, *Atmospheric Chemistry and Physics*,
616 10, 4909-4929, <https://doi.org/10.5194/acp-10-4909-2010>, 2010.

617 Sahu, L. K., Tripathi, N., Gupta, M., Singh, V., Yadav, R., Patel, K.: *Impact of*
618 *COVID-19 Pandemic lockdown in ambient concentrations of aromatic volatile organic*
619 *compounds in a metropolitan city of western India*, *Journal of geophysical research*,

620 Atmospheres : JGR, 127(6), <https://doi.org/10.1029/2022JD036628>, 2022.

621 Schauer, J., Kleeman, M., Cass, G., Simoneit, B.: Measurement of emissions from
622 air pollution sources.5. C₁-C₃₂ organic compounds from gasoline-powered motor
623 vehicles, Environmental Science & Technology, 36, 1169-1180,
624 <https://doi.org/10.1021/es0108077>, 2002.

625 Shao, P., An, J., Xin, J., Wu, F., Wang, J., Ji, D., and Wang, Y.: Source
626 apportionment of VOCs and the contribution to photochemical ozone formation during
627 summer in the typical industrial area in the Yangtze River Delta, China, Atmospheric
628 Research, 176-177, 64-74, <https://doi.org/10.1016/j.atmosres.2016.02.015>, 2016.

629 Singh, B., Sohrab, S., Athar, M., Alandijany, T., Kumari, S., Nair, A., Kumari, S.,
630 Mehra, K., Chowdhary, K., Rahman, S., Azhar, E.: Substantial changes in selected
631 volatile organic compounds (VOCs) and associations with health risk assessments in
632 industrial areas during the COVID-19 Pandemic, Toxics, 11, 165,
633 <https://doi.org/10.3390/toxics11020165>, 2023a.

634 Singh, B., Singh, M., Ulman, Y., Sharma, U., Pradhan, R., Sahoo, J., Padhi, S.,
635 Chandra, P., Koul, M., Tripathi, P., Kumar, D., Masih, J.: Distribution and temporal
636 variation of total volatile organic compounds concentrations associated with health risk
637 in Punjab, India, Case Studies in Chemical and Environmental Engineering, 8, 100417,
638 <https://doi.org/10.1016/j.cscee.2023.100417>, 2023b.

639 Song, M., Li, X., Yang, S., Yu, X., Zhou, S., Yang, Y., Chen, S., Dong, H., Liao,
640 K., Chen, Q., Lu, K., Zhang, N., Cao, J., Zeng, L., and Zhang, Y.: Spatiotemporal
641 variation, sources, and secondary transformation potential of volatile organic
642 compounds in Xi'an, China, Atmospheric Chemistry and Physics, 21, 4939-4958,
643 <https://doi.org/10.5194/acp-21-4939-2021>, 2021.

644 Song, X., Zhang, D., Li, X., Lu, X., Wang, M., Zhang, B., Zhang, R.: Simultaneous
645 observations of peroxyacetyl nitrate and ozone in Central China during static
646 management of COVID-19: Regional transport and thermal decomposition,
647 Atmospheric Research, Volume 294, 106958,
648 <https://doi.org/10.1016/j.atmosres.2023.106958>, 2023.

649 Song, Y., Shao, M., Liu, Y., Lu, S., Kuster, W., Goldan, P., and Xie, S.: Source
650 apportionment of ambient volatile organic compounds in Beijing, Environmental
651 Science & Technology, 41, 4348-4353, <https://doi.org/10.1021/es0625982>, 2007.

652 Wang, H., Wang, Q., Chen, J. Chen, C., Huang, C., Qiao, L. Lou, S., Lu, J.: Do
653 vehicular emissions dominate the source of C₆-C₈ aromatics in the megacity Shanghai

654 of eastern China?, *Environmental Science*, 27, 290-297, <https://doi.org/10.1016/j.jes.2014.05.033>, 2015.

656 Wang, M., Lu, S., Shao, M., Zeng, L., Zheng, J., Xie, F., Lin, H., Hu, K., and Lu,
657 X.: Impact of COVID-19 lockdown on ambient levels and sources of volatile organic
658 compounds (VOCs) in Nanjing, China, *Science of the Total Environment*, 757, 143823,
659 <https://doi.org/10.1016/j.scitotenv.2020.143823>, 2021.

660 Wang, M., Zeng, L., Lu, S., Shao, M., Liu, X., Yu, X., Chen, W., Yuan, B., Zhang,
661 Q., Hu, M., & Zhang, Z.: Development and validation of a cryogen-free automatic gas
662 chromatograph system (GC-MS/FID) for online measurements of volatile organic
663 compounds, *Analytical Methods*, 6, 9424, <https://doi.org/10.1039/C4AY01855A>, 2014.

664 Wang, T., Xue, L., Brimblecombe, P., Lam, Y. F., Li, L., and Zhang, L.: Ozone
665 pollution in China: A review of concentrations, meteorological influences, chemical
666 precursors, and effects, *Science of the Total Environment*, 575, 1582-1596,
667 <https://doi.org/10.1016/j.scitotenv.2016.10.081>, 2017.

668 Wu, R., Li, J., Hao, Y., Li, Y., Zeng, L., and Xie, S.: Evolution process and sources
669 of ambient volatile organic compounds during a severe haze event in Beijing, China,
670 *Science of the Total Environment*, 560-561, 62-72,
671 <https://doi.org/10.1016/j.scitotenv.2016.04.030>, 2016.

672 Wu, W., Zhao, B., Wang, S., and Hao, J.: Ozone and secondary organic aerosol
673 formation potential from anthropogenic volatile organic compounds emissions in China,
674 *Journal of Environmental Sciences*, 53, 224-237,
675 <https://doi.org/10.1016/j.jes.2016.03.025>, 2017.

676 Xiong, Y., Zhou, J., Xing, Z., and Du, K.: Optimization of a volatile organic
677 compound control strategy in an oil industry center in Canada by evaluating ozone and
678 secondary organic aerosol formation potential, *Environmental Research*, 191, 110217,
679 <https://doi.org/10.1016/j.envres.2020.110217>, 2020.

680 Yun, L., Li, C., Zhang, M., He, L. and Guo, J.: Pollution characteristics and sources
681 of atmospheric VOCs in the coastal background area of the Pearl River Delta,
682 *Environmental Science*, 4191-4201, <https://doi.org/10.13227/j.hjlx.202101155>, 2021.

683 Zeng, X., Han, M., Ren, G., Liu, G., Wang, X., Du, K., Zhang, X., and Lin, H.: A
684 comprehensive investigation on source apportionment and multi-directional regional
685 transport of volatile organic compounds and ozone in urban Zhengzhou, *Chemosphere*,
686 334, 139001, <https://doi.org/10.1016/j.chemosphere.2023.139001>, 2023.

687 Zhang, C., Liu, X., Zhang, Y., Tan, Q., Feng, M., Qu, Y., An, J., Deng, Y., Zhai, R.,

688 Wang, Z., Cheng, N., and Zha, S.: Characteristics, source apportionment and chemical
689 conversions of VOCs based on a comprehensive summer observation experiment in
690 Beijing, *Atmospheric Pollution Research*, 12, 230-241,
691 <https://doi.org/10.1016/j.apr.2020.12.010>, 2021a.

692 Zhang, D., He, B., Yuan, M., Yu, S., Yin, S., and Zhang, R.: Characteristics,
693 sources and health risks assessment of VOCs in Zhengzhou, China during haze
694 pollution season, *Journal of Environmental Sciences*, 108, 44-57,
695 <https://doi.org/10.1016/j.jes.2021.01.035>, 2021b.

696 Zhang, F., Shang, X., Chen, H., Xie, G., Fu, Y., Wu, D., Sun, W., Liu, P., Zhang,
697 C., Mu, Y., Zeng, L., Wan, M., Wang, Y., Xiao, H., Wang, G., and Chen, J.: Significant
698 impact of coal combustion on VOCs emissions in winter in a North China rural site,
699 *Science of the Total Environment*, 720, 137617,
700 <https://doi.org/10.1016/j.scitotenv.2020.137617>, 2020.

701 Zhang, J., Sun, Y., Wu, F., Sun, J., and Wang, Y.: The characteristics, seasonal
702 variation and source apportionment of VOCs at Gongga Mountain, China, *Atmospheric
703 Environment*, 88, 297-305, <https://doi.org/10.1016/j.atmosenv.2013.03.036>, 2014.

704 Zhang, Z., Yan, X., Gao, F., Thai, P., Wang, H., Chen, D., Zhou, L., Gong, D., Li,
705 Q., Morawska, L., and Wang, B.: Emission and health risk assessment of volatile
706 organic compounds in various processes of a petroleum refinery in the Pearl River Delta,
707 China, *Environmental Pollution*, 238, 452-461,
708 <https://doi.org/10.1016/j.envpol.2018.03.054>, 2018.

709 Zheng, H., Kong, S., Xing, X., Mao, Y., Hu, T., Ding, Y., Li, G., Liu, D., Li, S.,
710 and Qi, S.: Monitoring of volatile organic compounds (VOCs) from an oil and gas
711 station in northwest China for 1 year, *Atmospheric Chemistry and Physics*, 18, 4567-
712 4595, <https://doi.org/10.5194/acp-18-4567-2018>, 2018.

713 Zheng, J., Zhong, L., Wang, T., Louie, P. K. K., and Li, Z.: Ground-level ozone in
714 the Pearl River Delta region: Analysis of data from a recently established regional air
715 quality monitoring network, *Atmospheric Environment*, 44, 814-823,
716 <https://doi.org/10.1016/j.atmosenv.2009.11.032>, 2010.

717 Zhou, Z., Xiao, L., Fei, L., Yu, W., Lin M., Huang, T., Zhang, Z. and Tao J.:
718 Characteristics and sources of VOCs during ozone pollution and non-pollution periods
719 in summer in Dongguan industrial concentration area, *Environmental Science*, 4497-
720 4505, <https://doi.org/10.13227/j.hjcx.202111285>, 2022.

721 Zou, Y., Yan, X. L., Flores, R. M., Zhang, L. Y., Yang, S. P., Fan, L. Y., Deng, T.,

722 Deng, X. J., and Ye, D. Q.: Source apportionment and ozone formation mechanism of
723 VOCs considering photochemical loss in Guangzhou, China, *Science of the Total*
724 *Environment*, 903, 166191, <https://doi.org/10.1016/j.scitotenv.2023.166191>, 2023.

725 Zuo, H., Jiang, Y., Yuan, J., Wang, Z., Zhang, P., Guo, C., Wang, Z., Chen, Y., Wen,
726 Q., Wei, Y., Li, X.: Pollution characteristics and source differences of VOCs before and
727 after COVID-19 in Beijing, *Science of The Total Environment*, 907, 167694,
728 <https://doi.org/10.1016/j.scitotenv.2023.167694>, 2024.

729